

## Semirotaxanes and unsymmetrical rotaxanes from substituted benzylammonium salts and dibenzo-24-crown-8

Zhenbin Niu, Amy L. Fletcher, Carla Slebodnick, and Harry W. Gibson\*

Department of Chemistry, Virginia Tech, Blacksburg, Virginia 24060, USA  
[hwgibson@vt.edu](mailto:hwgibson@vt.edu)

This paper is dedicated to Prof. Phil Hodge in honor of his creative and diverse research career in organic and polymer chemistry that has been an inspiration to the senior author

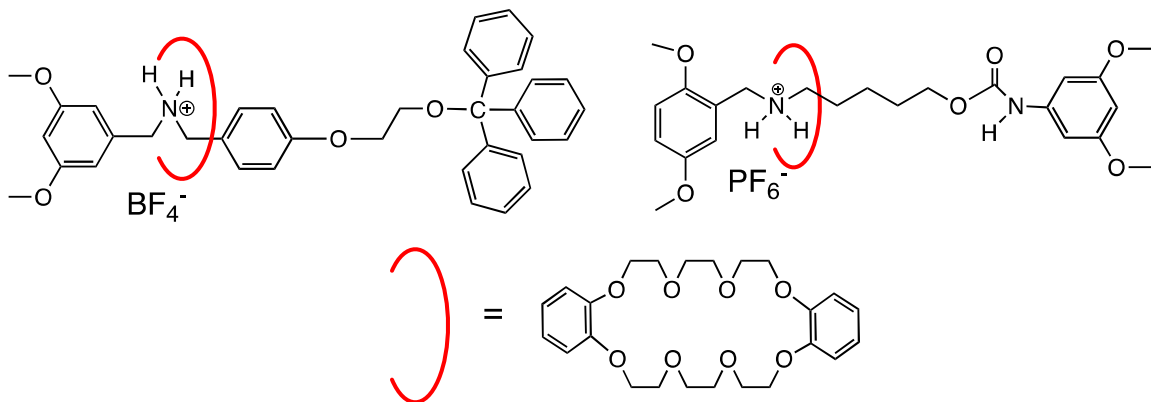
Received 12-18-2020

Accepted 02-17-2021

Published on line 02-21-2021

### Abstract

Three new hydroxyl-functionalized secondary benzyl ammonium salts were synthesized and complexed with dibenzo-24-crown-8. Three [2]semirotaxanes and then their two [2]rotaxanes each with two different stoppers were prepared successfully by reactions of the hydroxyl groups with bulky reagents. X-ray analysis of a single crystal of a [2]semirotaxane confirmed its structure. The formation of the [2]semirotaxanes can be reversibly controlled by adding  $KPF_6$  and 18-crown-6 sequentially. These new unsymmetrical [2]rotaxanes afford a way to prepare planar chiral rotaxanes and related supramolecular systems.



**Keywords:** Semirotaxane, rotaxane, self-assembly, supramolecular chemistry

## Introduction

In supramolecular chemistry, pseudorotaxanes,<sup>1-5</sup> which consist of linear molecular components (“guests”) threaded through macrocyclic components (“hosts”), are key building blocks for more sophisticated constructs, including polymeric analogs.<sup>6-12</sup> In solution the linear guest dethreads and rethreads as a result of the dynamic equilibrium between the pseudorotaxane and its two components. If a bulky stopper, whose size is bigger than the central cavity of the cyclic host, is applied to one end of the linear guest, a semirotaxane is afforded (Figure 1). If bulky stoppers are attached at both ends of the linear guest, a rotaxane is formed. Similar to pseudorotaxanes, semirotaxanes are important parts of supramolecular chemistry research because this is the route to mechanically interlocked systems that cannot dethread without covalent bond cleavage. Such interlocked structures have been widely used in molecular machines<sup>12-24</sup> and systems that can be controlled by external stimuli,<sup>25,26</sup> such as electrochemistry,<sup>27,28</sup> pH,<sup>28-31</sup> etc.<sup>32,33</sup>

It has been known for more than two decades that dibenzo-24-crown-8 (**DB24C8**) and its derivatives form stable pseudorotaxanes with secondary ammonium salts driven by hydrogen bonding and ion-dipole interactions in low-polarity solvents,<sup>34,35</sup> such as acetone and acetonitrile. These systems have been widely employed in the preparation of pseudorotaxanes, rotaxanes and catenanes. The conversion of pseudorotaxanes to rotaxanes must always proceed via the semirotaxane, but this is often done in one step using an excess of the stoppering agent.

We became interested in construction of rotaxanes with unsymmetrical guests, i. e., bearing two different stoppers. Such rotaxanes can be chiral if the host is unsymmetrically substituted.<sup>36-39</sup> This is exemplified in Figure 2. This is an intriguing prospect as a means of controlling/varying stereochemical properties.

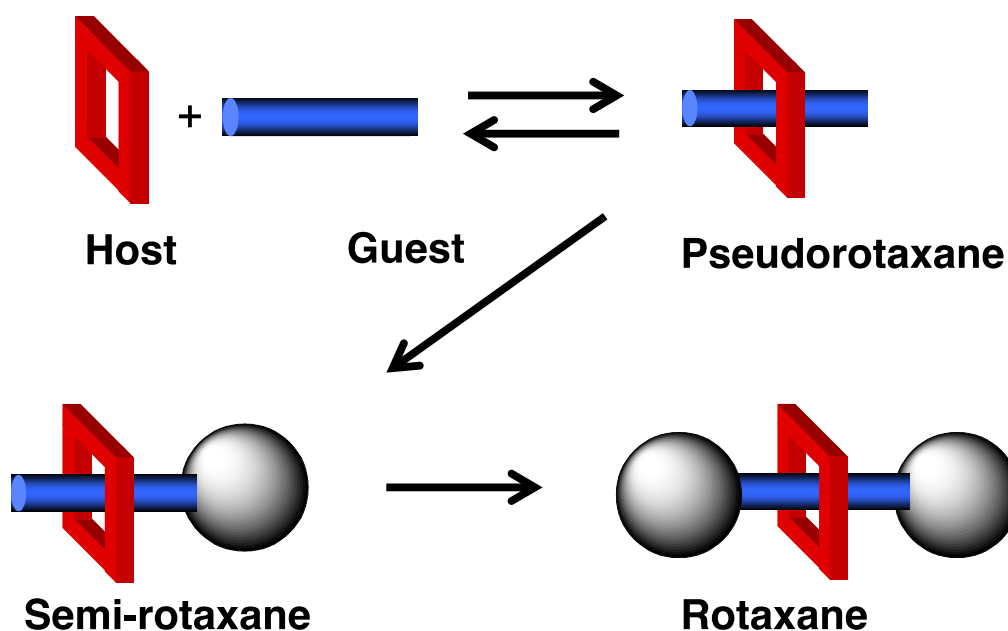


**Figure 1.** Cartoon representations of a pseudorotaxane, a semirotaxane and a rotaxane.

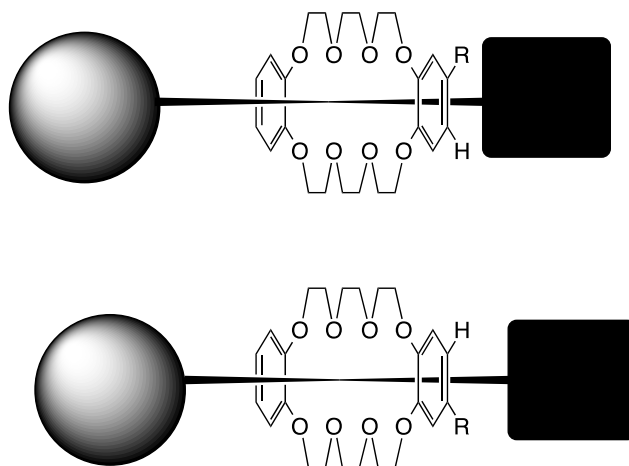


**Figure 2.** Cartoon representation of the enantiomers of a planar chiral DB24C8-based rotaxane.

Thermodynamically controlled self-assembly is a desirable approach for rotaxane synthesis that takes advantage of a labile bond between the guest molecule and the end stopper groups. The reversibility of this bond allows for threading by the host molecule via chemical equilibrium. If the stoppering reactions are reversible, the yield of the rotaxane is dependent solely upon its stability in relation to all the other components in the mixture. Figure 3 illustrates this approach in a cartoon schematic.

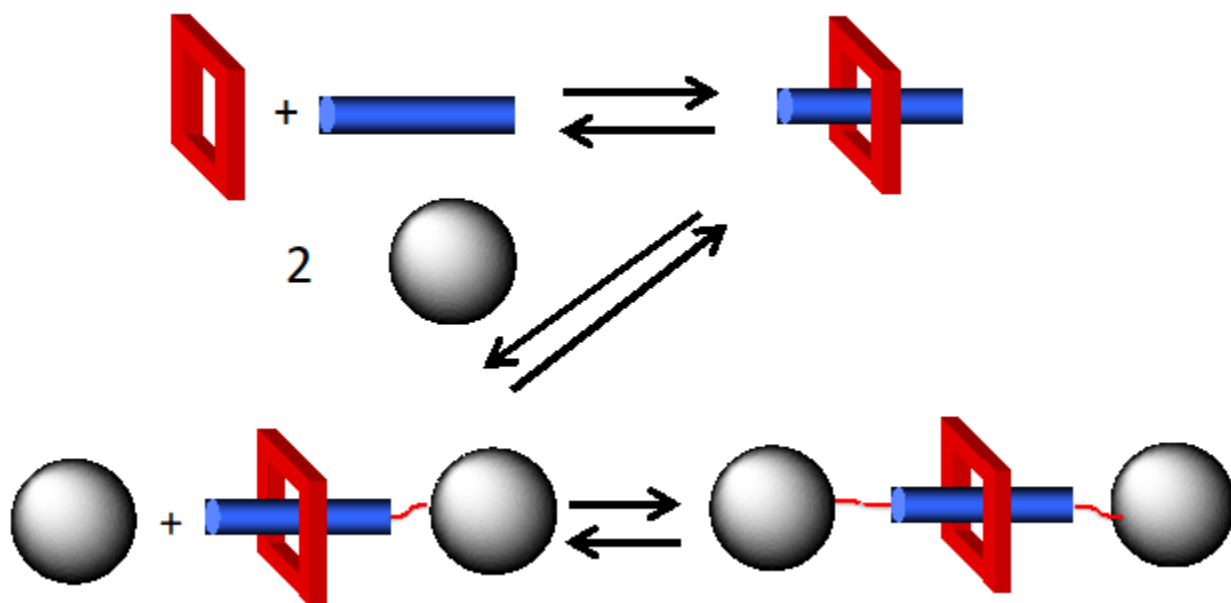


**Figure 3.** Cartoon representation of reversible attachment of stoppers. If the rotaxane is the lowest energy species, it will be thermodynamically favored.

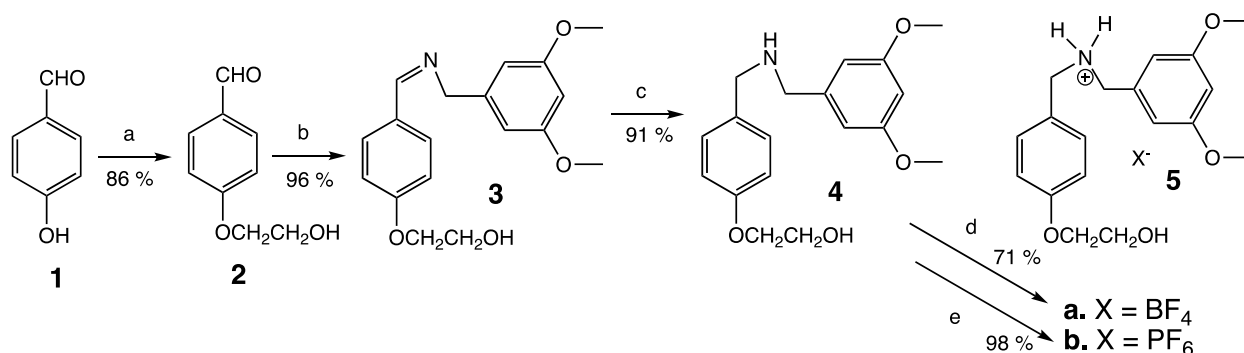
Stoddart and co-workers used reversible imine bond-formation and other methods to construct so-called dynamic [2]rotaxanes.<sup>40-42</sup> Takata and co-workers reported the thermodynamic synthesis of rotaxanes based on reversible tritylative endcapping of pseudorotaxanes having thiol or hydroxyl functionality<sup>43,44</sup> and reversible thiol-disulfide reactions.<sup>45,46</sup> Similar work with endcapping was published Tokunaga et al.<sup>47</sup>

In the present work, new hydroxyl-functionalized secondary ammonium salts were synthesized and complexed with dibenzo-24-crown-8 to form semirotaxanes and thence converted to [2]rotaxanes. The hydroxyl group of one of the guest species was endcapped via tritylation to form a thermodynamically stable unsymmetrical [2]rotaxane.

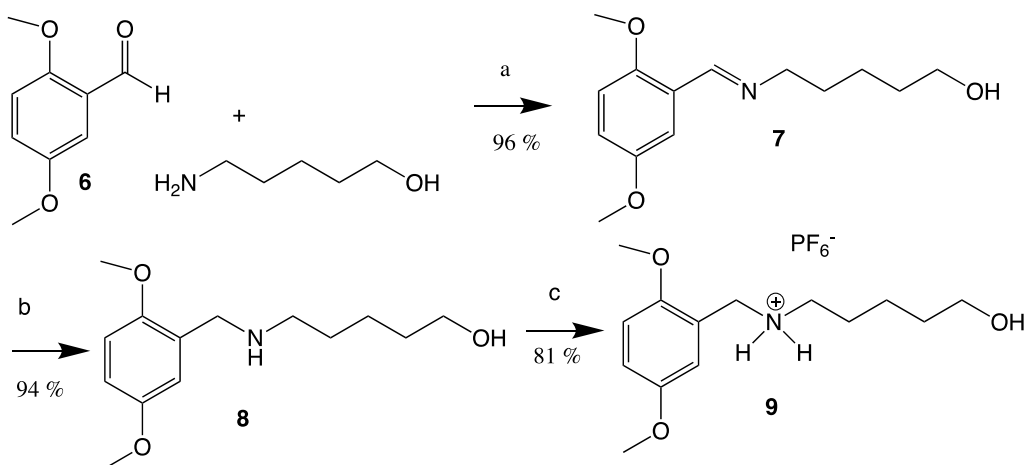
## Results and Discussion

### Ammonium salts

Guests **5** and **9** were designed as model components for planar chiral supramolecular structures. The new ammonium salts **5** and **9** were synthesized via efficient, multi-step reaction sequences: first imine formation from the corresponding aldehydes **2** and **6** with amines, then reduction of the imines **3** and **7** to secondary amines **4** and **8**, which in turn were converted to the secondary ammonium salts by standard methods (Schemes 1 and 2). Their structures were confirmed by NMR spectroscopy, mass spectrometry and elemental analysis.



**Scheme 1.** Syntheses of *p*-(2'-hydroxyethoxy)benzyl-3'',5''-dimethoxybenzylammonium tetrafluoroborate (**5a**) and hexafluorophosphate (**5b**): a) 2-chloroethanol, K<sub>2</sub>CO<sub>3</sub>, ethanol, reflux; b) 3,5-dimethoxybenzyl amine, TsOH, toluene, Dean-Stark trap, reflux; c) NaBH<sub>4</sub>, methanol, reflux; d) HBF<sub>4</sub>, ether, rt; e) HCl, rt then NH<sub>4</sub>PF<sub>6</sub>/H<sub>2</sub>O.



**Scheme 2.** Synthesis of 2,5-dimethoxybenzyl-5'-hydroxypentylammonium hexafluorophosphate (**9**): a) TsOH, toluene, Dean-Stark trap, reflux; b) NaBH<sub>4</sub>, methanol, rt; c) HCl, ethyl acetate, then NH<sub>4</sub>PF<sub>6</sub>/H<sub>2</sub>O, rt.

A single crystal of salt **9** was subjected to X-ray crystallographic analysis, which indicates a quasi-planar structure in which the aminoalcohol substituent adopts the expected linear zig-zag conformation (Figure 4). Hydrogen bonds between a fluorine atom of the PF<sub>6</sub> counterion with both N-H protons of the ammonium ion (**b** and **c**) and a benzylic C-H proton bonding to the same fluorine (**d**) coupled with an inter-ion bond between the ether oxygen of the 2-methoxy moiety (**a**) and an N-H proton hold the cation in a relatively rigid conformation.

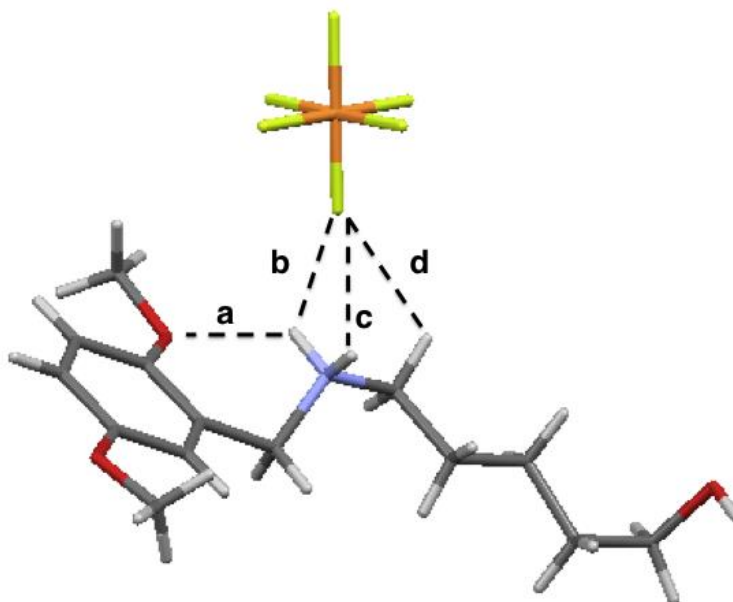


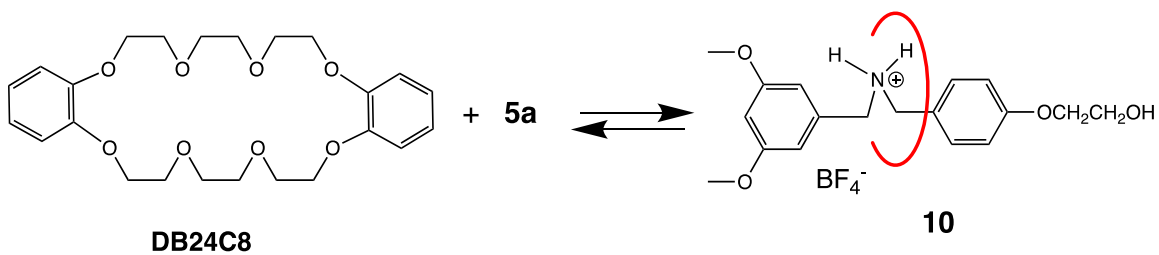
**Figure 4.** X-ray crystal structure of ammonium salt **9**. Distance/Angle **a**: O----H 2.11 Å, O----H-N angle 128 °; **b**: H----F 2.17 Å, N-H----F 124 °; **c**: H----F 2.85 Å, N-H----F 77.3 °; **d**: H----F 2.59 Å, C-H----F 112 °.

### Semirotaxanes

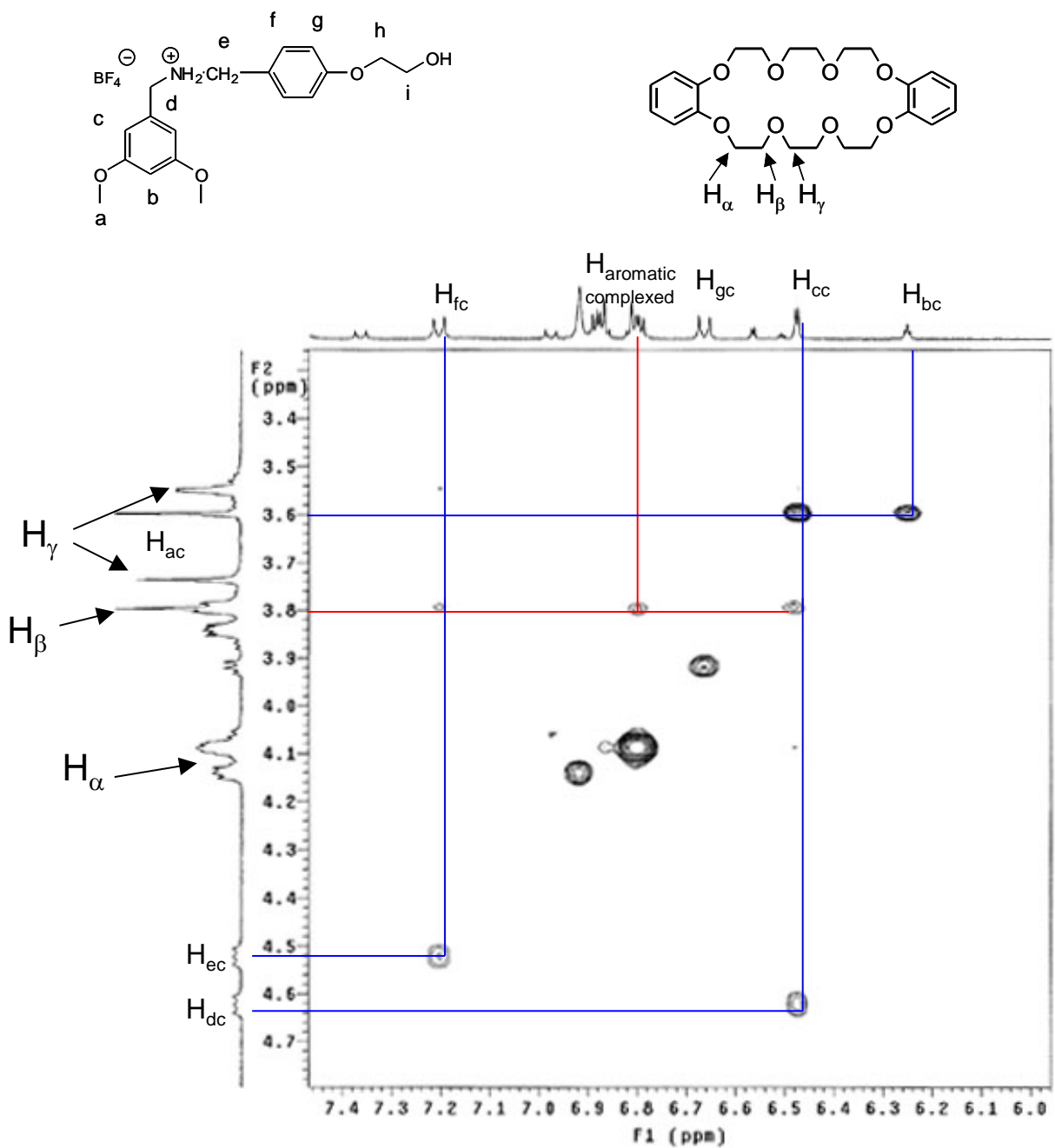
There are two different extremes of exchange rates for complexation relative to the <sup>1</sup>H NMR time scale: fast and slow exchange. In fast exchange only one peak is observed for each non-equivalent proton in the host and guest; it is a time-averaged signal of the complexed and uncomplexed species. In the fast exchange regime, association constants are calculated by using the change in chemical shifts. In slow exchange complexation, two signals are observed for each non-equivalent proton. One signal is observed for each non-equivalent proton in the uncomplexed species and new signals correspond to the complexed species. The relative concentrations of uncomplexed and complexed species can thus be calculated using peak integration values in some cases.<sup>48,49</sup>

#### a. Semirotaxane **10** from DB24C8 and secondary ammonium BF<sub>4</sub> salt **5a**

The new salt **5a** was complexed with dibenzo-24-crown-8 (**DB24C8**) (Scheme 3). The expected COSY correlations for the starting materials were observed (see SM, Figures S21 and S22). Then a solution of **DB24C8** and **5a** was subjected to the NOESY protocol. Figure 5 shows the partial NOESY NMR spectrum of the slow exchange system. In addition to the COSY correlations for H<sub>ec</sub> with H<sub>fc</sub>, and H<sub>dc</sub> with H<sub>cc</sub>, and H<sub>cc</sub> with H<sub>bc</sub>, two important NOESY correlations occur for H<sub>fc</sub> (7.2 ppm) with H<sub>βc</sub> (3.8 ppm), and H<sub>cc</sub> (6.5 ppm) with H<sub>bc</sub> (3.8 ppm). These through-space couplings of the β-protons of the complexed crown ether with the aromatic protons of the complexed guest demonstrate the formation of semirotaxane **10**.

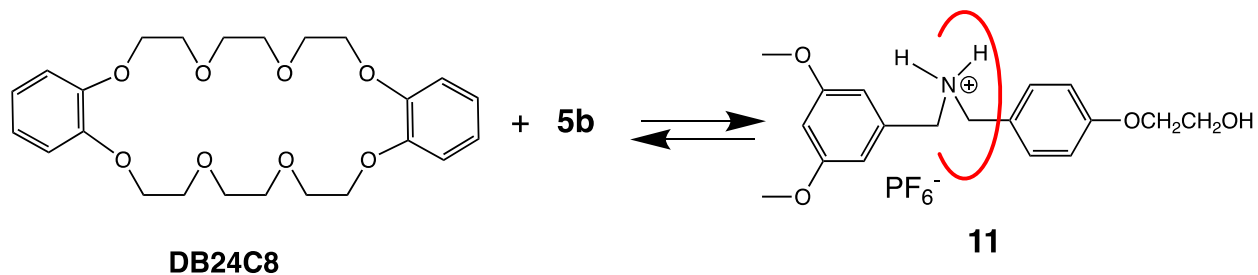


**Scheme 3.** Synthesis of semirotaxane **10** from host **DB24C8** and guest **5a**.



### b. Semirotaxane **11** from **DB24C8** and secondary ammonium $\text{PF}_6^-$ salt **5b**

The complexation of **5b** with **DB24C8** (Scheme 4) was studied via NMR spectroscopy (Figure 6), which revealed slow exchange in  $\text{CD}_3\text{CN}$ . One method for analysis of slow exchange systems is the single point method. This method is not always an appropriate method, however; if the complex is not ion paired and the guest salt is ion paired, detailed studies as a function of concentration are required, as noted previously.<sup>48,49</sup> In the case of **11** an apparent association constant was determined by integration of the complexed and uncomplexed  $\gamma$ -proton signals of **DB24C8** and the complexed and uncomplexed aromatic protons of the guest species ( $\text{H}_f$  and  $\text{H}_{fc}$ ) in 10 mM solutions of host and guest: average  $K_{a\text{exp}}$   $(1.1 \pm 0.4) \times 10^2 \text{ M}^{-1}$  (see SM, Figure S16). This relatively low  $K_a$  value can be attributed to the electron donating quality of the *p*-hydroxyethoxy moiety.



**Scheme 4.** Synthesis of semirotaxane **11** in  $\text{CD}_3\text{CN}$  from host **DB24C8** and guest **5b**.

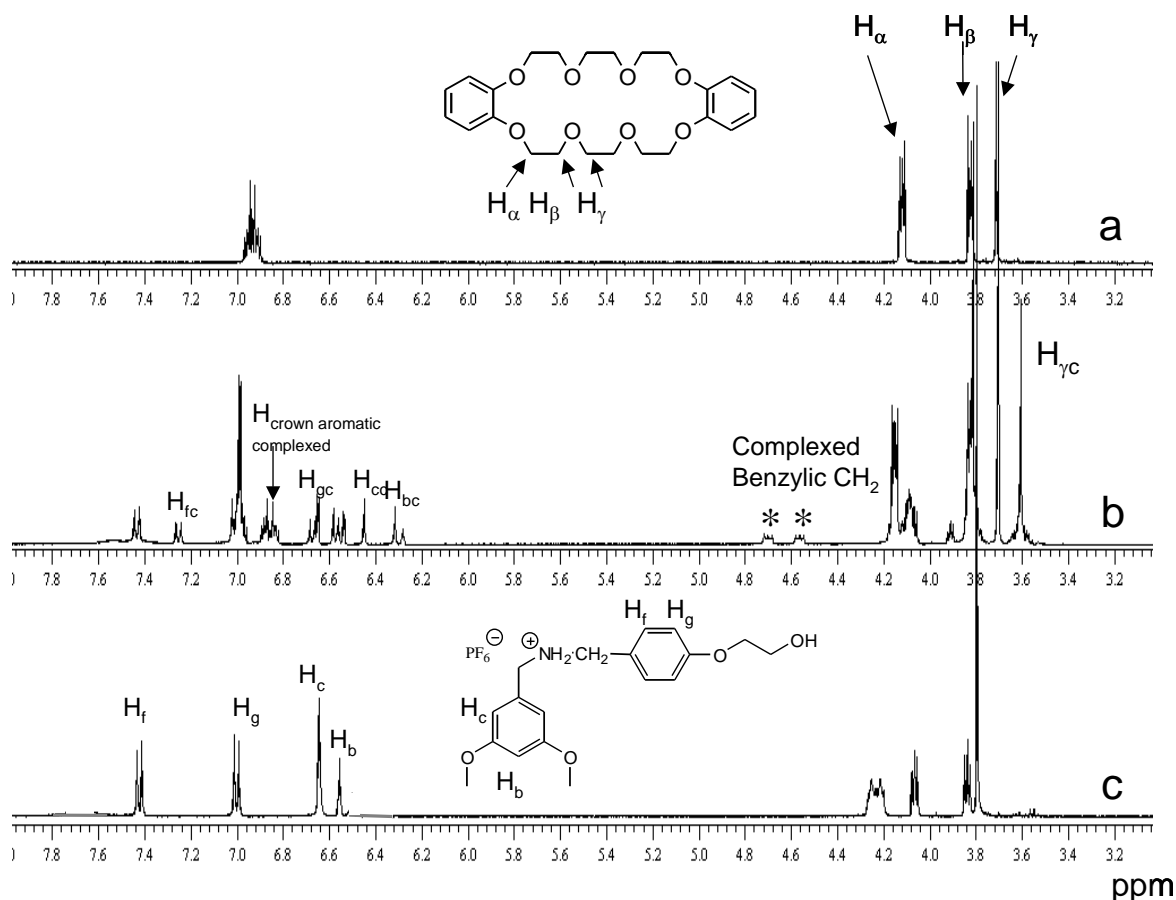
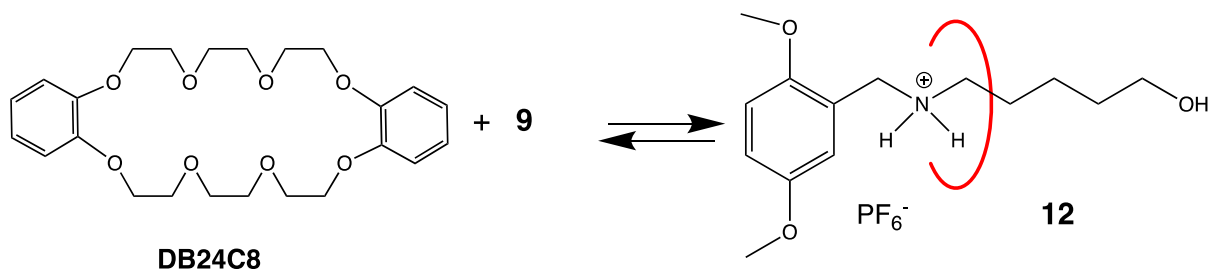


**Figure 6.** Stacked  $^1\text{H}$  NMR spectra ( $\text{CD}_3\text{CN}$ , 400 MHz, ambient T) of a) **DB24C8**; b) **DB24C8** + **5b** (10 mM each); and c).

### c. Semirotaxane **12** from **DB24C8** and secondary ammonium $\text{PF}_6^-$ salt **9**

The complexation of **DB24C8** with **9** was studied by  $^1\text{H-NMR}$ . Upon mixing **9** and **DB24C8** in acetone- $d_6$  (Scheme 5), the signal corresponding to proton  $\text{H}_\gamma$  shifted upfield, whereas signals of  $\text{H}_1$ ,  $\text{H}_\alpha$  and  $\text{H}_\beta$  shifted downfield (Figure 7). It is noteworthy that in contrast to the slow exchange observed for dibenzyl ammonium-based semirotaxanes **10** and **11**, here the complexation dynamics are fast; this is probably due the contrasting benzyl-*n*-pentyl ammonium guest structure, which provides less steric hindrance for threading and dethreading. These observations indicated that stable complex **12** between **9** and **DB24C8** had formed. The ESI-MS confirmed the formation of the [2]semirotaxane **12** (see SM, Figure S18). A peak corresponding to  $[\text{M-PF}_6]^+$  was found. No other related peaks were observed.



**Scheme 5.** Synthesis of semirotaxane **12** from host **DB24C8** and guest **9**.

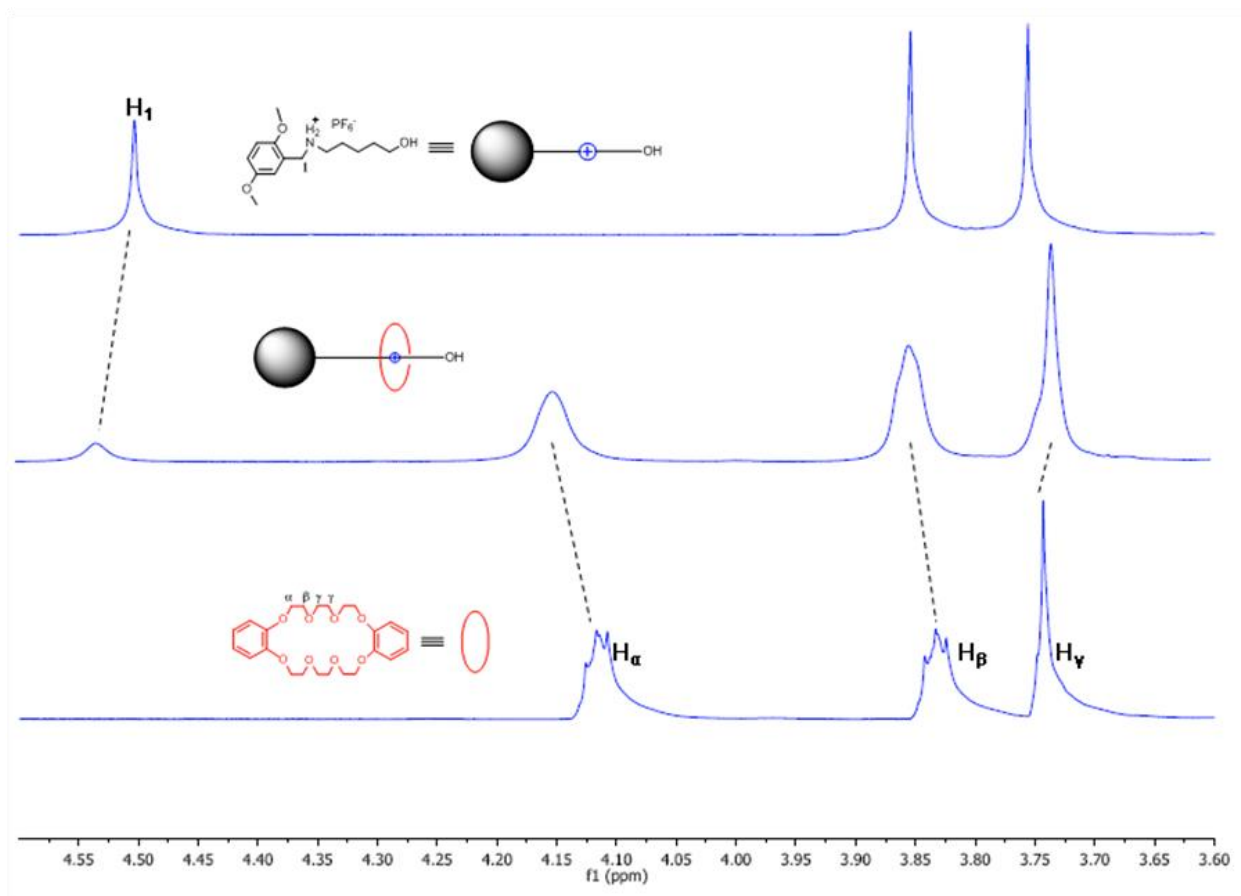


**Figure 7.** Partial  $^1\text{H-NMR}$  spectra (400 MHz, acetone- $d_6$ , 25 °C) of **DB24C8** (bottom), equimolar solution of **DB24C8** and ammonium salt **9** (middle) and guest **9** (upper).



Similar to the other reported dibenzo crown/secondary ammonium salt-based pseudorotaxanes,<sup>50</sup> the complexation was controlled by alternately adding  $\text{KPF}_6$  and 18-crown-6 (**18C6**) to the solution. As shown in Figure 8, when excess  $\text{KPF}_6$  was added to a solution of **9** and **DB24C8**, the [2]semirotaxane **12** was dissociated.  $\text{H}_1$  shifted upfield to the position corresponding to that of free **9** and  $\text{H}_\alpha$ ,  $\text{H}_\beta$  and  $\text{H}_\gamma$  shifted to the positions corresponding to those of unbound **DB24C8**. Then when **18C6** was added, [2]semirotaxane **12** was regenerated and all the peaks shifted back to their original positions. This is due to the facts that 1) **DB24C8** binds  $\text{KPF}_6$  much more strongly than ammonium salt **9**, but 2) **18C6** in turn binds  $\text{KPF}_6$  very strongly, but does not interact strongly with ammonium salt **9**.<sup>50</sup>

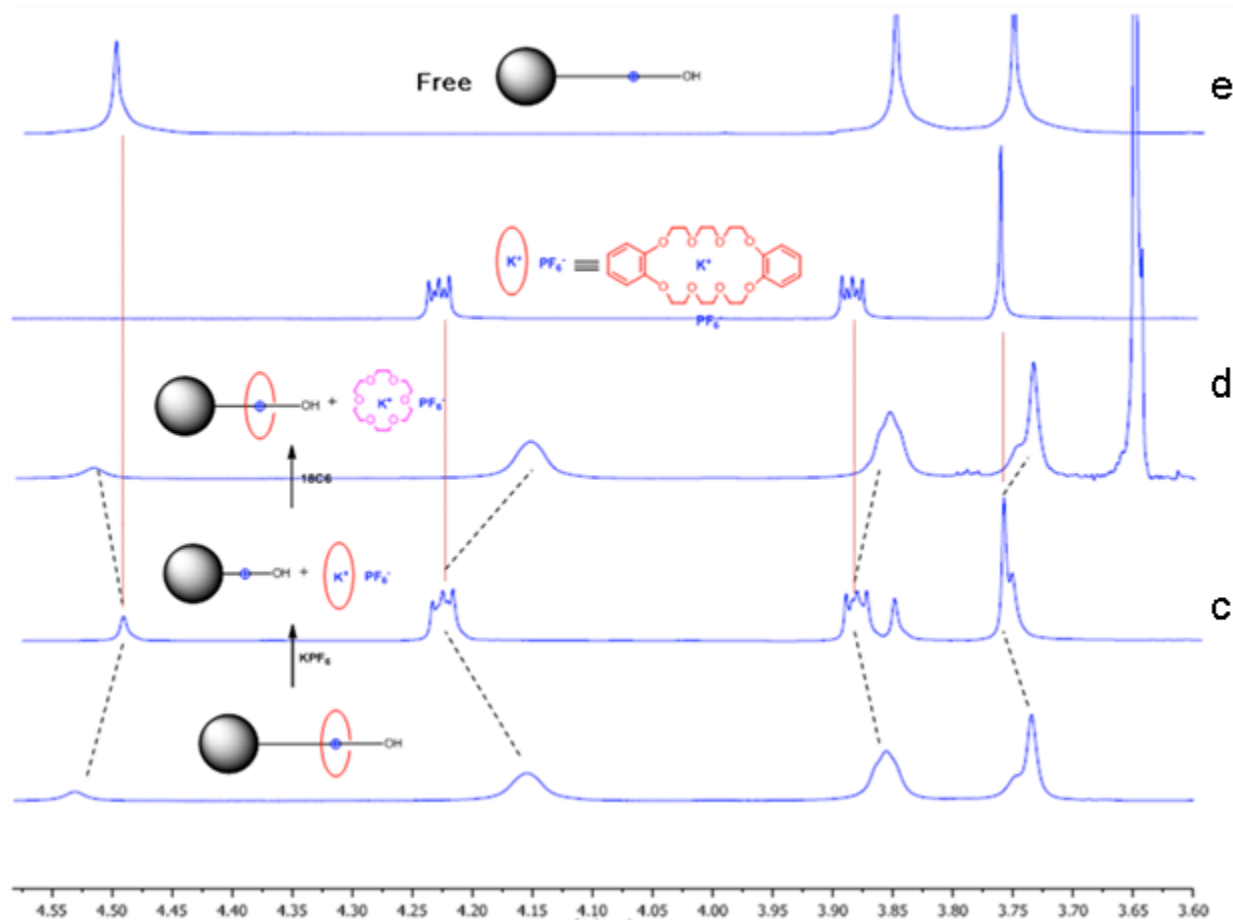


**Figure 8.** Partial  $^1\text{H}$  NMR spectra (400 MHz, acetone- $d_6$ , 25 °C) a) equimolar (1 mM) solution of **DB24C8** and **9**. b) prior solution after addition of  $\text{KPF}_6$  (1.2 equiv). c) prior solution after addition of **18C6** (1.2 equiv). d) equimolar **DB24C8** and  $\text{KPF}_6$ . e) guest **9**.

X-ray analysis of a single crystal of the semirotaxane complex **12** (Figure 9) indicates that it is stabilized by hydrogen bonds between the oxygen atoms of host **DB24C8** and the NH protons as well as the benzylic protons of guest **9**. As expected, the bulky dimethoxyphenyl unit is much larger than the cavity of **DB24C8**. Therefore, if another bulky stopper is applied to the hydroxyl end of the linear guest in the semirotaxane, a [2]rotaxane will be formed.

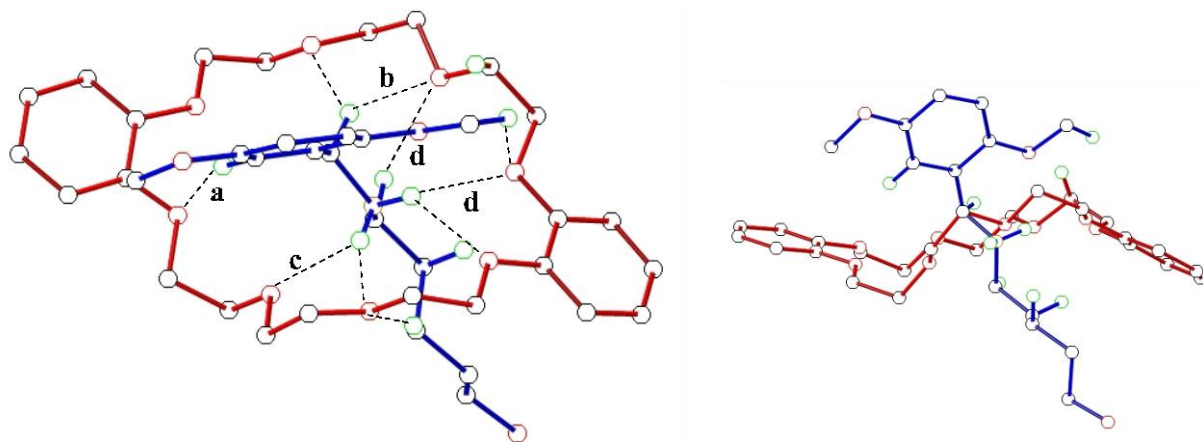
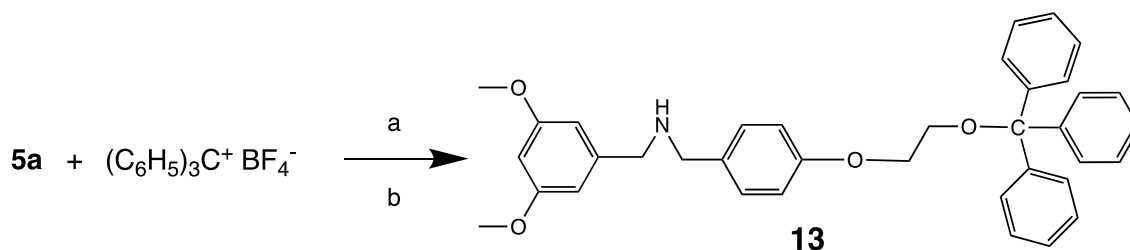


**Figure 9.** Two views of the X-ray structure of semirotaxane **12**. **DB24C8** is red. **9** is blue. Hydrogen atoms are green. Solvent molecules, minor disordered carbon and hydrogen atoms, except the ones involved in hydrogen bonding, have been omitted for clarity. Hydrogen bonds in the right hand structure were omitted for clarity. Selected hydrogen-bond parameters: H $\cdots$ O(N) distances (Å), C $\cdots$ O(N) distances (Å), C-H $\cdots$ O(N) angles (deg): a 2.705, 3.586, 154.5; b 2.569, 3.374, 138.4; c 2.264, 2.980, 134.3; d 2.328, 3.177, 153.2.

## [2]Rotaxanes

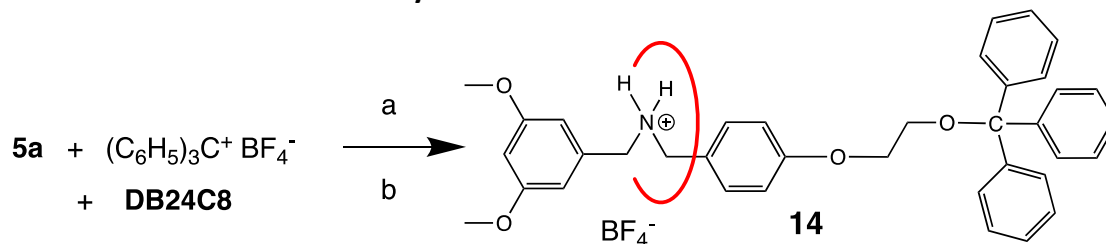
### a. Model tritylation

The model reaction was conducted using the  $\text{BF}_4^-$  salt **5a** and trityl tetrafluoroborate to form the second stopper group (Scheme 6). The product was isolated as a white solid in a disappointing 39% yield, which most likely could be improved by use of a weaker base.<sup>43</sup> Figure 10 shows the  $^1\text{H}$  NMR spectrum of model dumbbell **13**.



**Scheme 6.** Synthesis of trityl ether **13**: a) 1/1  $\text{CHCl}_3/\text{CH}_3\text{CN}$ , rt, 24 h; b) 10% NaOH (aq.) wash; 39%.

### b. Rotaxane **14** from **DB24C8** and secondary ammonium salt **5a**



**Scheme 7.** Synthesis of [2]rotaxane **14** from **DB24C8** and guest **5a**: a) 1/1  $\text{CHCl}_3/\text{CH}_3\text{CN}$ , rt, 24 h; b) 10% NaOH (aq.) wash; 32%.

The synthesis of the rotaxane **14** was conducted in the same way using the  $\text{BF}_4$  salt **5a**, **DB24C8**, and trityl tetrafluoroborate. Figure 10 shows the  $^1\text{H}$  NMR spectra of **13**, **14**, and **DB24C8**. Note that the workup involved washing with base to halt the equilibration process and permanently install the trityl end group as with model dumbbell **13**; however, in the case of the rotaxane, treatment with base does not lead to deprotonation as demonstrated in similar systems.<sup>51</sup> The benzylic proton signals are shifted downfield from the amine **13** as in the semirotaxane **10** (Figure 6), indicating that the guest is still protonated. Small signals at 7.50, 7.02 and 6.61 ppm indicate that dumbbell **13** was present as an impurity. However, the rotaxane structure was confirmed by mass spectrometry (see SM, Figure S20).

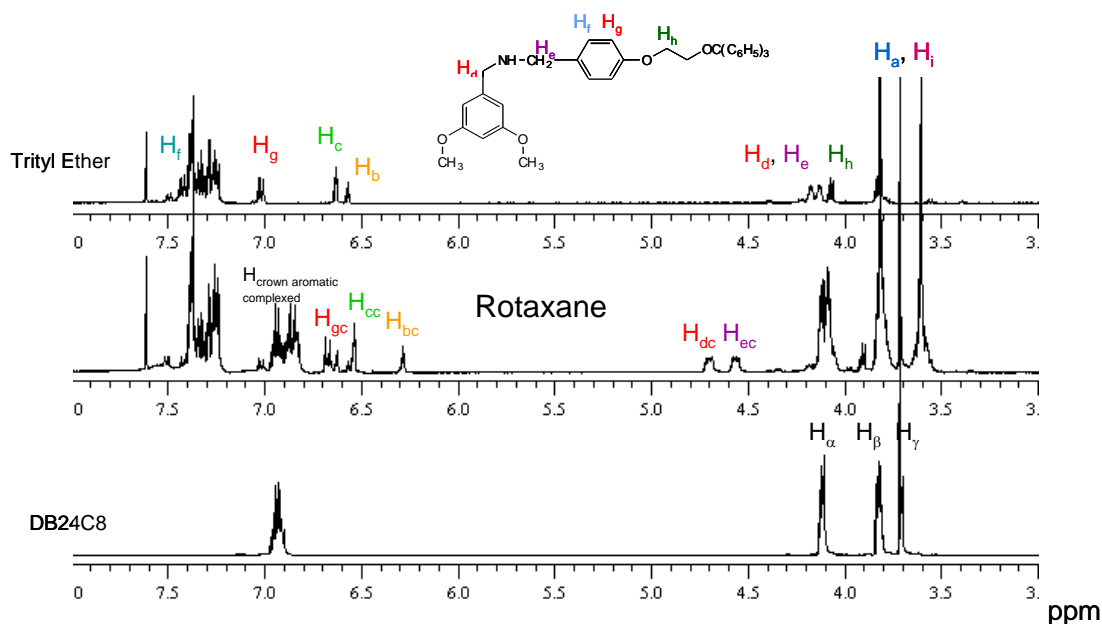


**Figure 10.** Stacked  $^1\text{H}$  NMR spectra ( $\text{CD}_3\text{CN}$ , 400 MHz, ambient T) of trityl ether **13**, rotaxane **14**, and **DB24C8**.

After determining the COSY correlations (see SM, Figure S23), a NOESY spectrum was obtained for rotaxane **14** (Figure 11). In addition to the COSY correlations, through-space correlations occur between  $\text{H}_\beta$  of the crown ether (3.8 ppm) with  $\text{H}_f$  (7.2 ppm) and with  $\text{H}_c$  (6.5 ppm) of the linear guest. Since here there are no uncomplexed signals and these couplings are identical to those observed for the complexed signals corresponding to semirotaxane **10** (Figure 6), this spectrum proves that this compound is indeed a rotaxane.

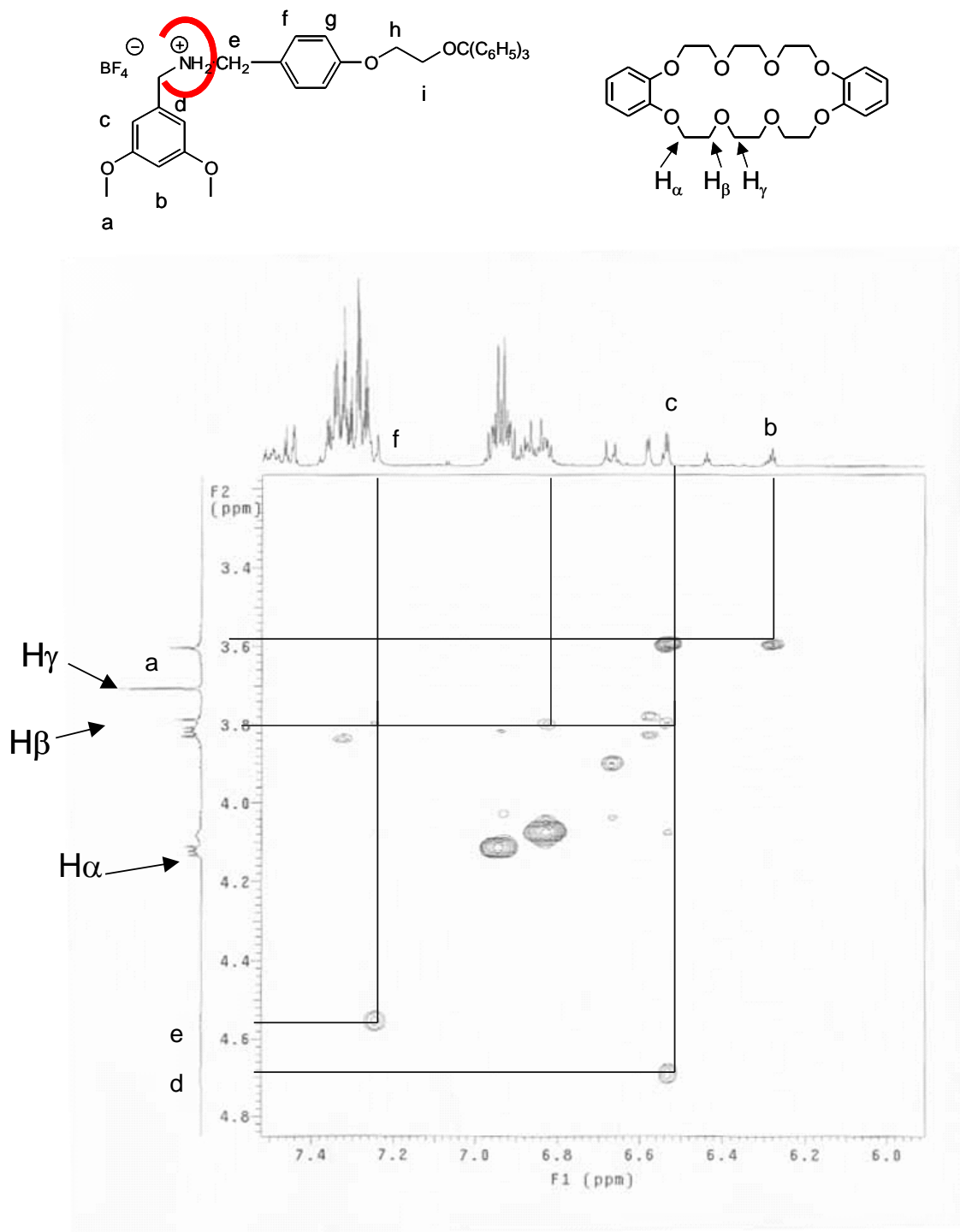
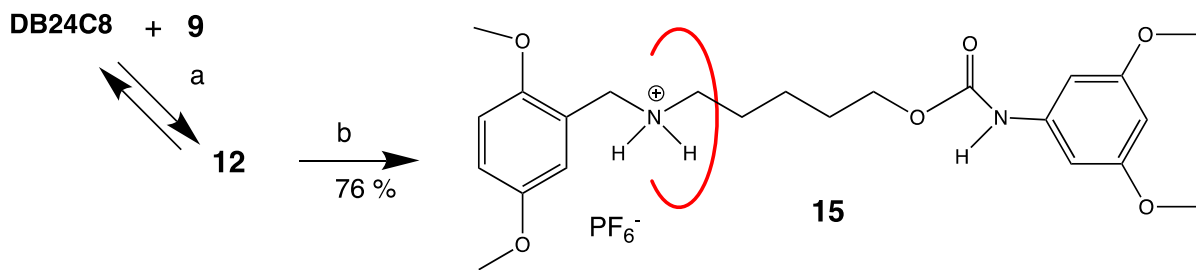


**Figure 11.** Partial NOESY  $^1\text{H}$  NMR spectrum of rotaxane **14** (2/3  $\text{CD}_3\text{CN}/\text{CDCl}_3$ , 400 MHz, 23  $^\circ\text{C}$ ).

### c. Rotaxane **15** from **DB24C8** and **9**

An equimolar mixture of **9** and **DB24C8** in dry dichloromethane (DCM) was treated with 3,5-dimethoxyphenyl isocyanate (Scheme 8). After purification, [2]rotaxane **15** was obtained as a waxy solid, whose structure was confirmed by mass spectrometry (see SM, Figure S25).



**Scheme 8.** Synthesis of [2]rotaxane **15** from **DB24C8** and guest **9** by *in situ* stoppering of semirotaxane **12**: a) dry  $\text{CH}_2\text{Cl}_2$  (DCM), b) 3,5-dimethoxyphenyl isocyanate, di(*n*-butyl)tin dilaurate, 23 °C, 2 days.

The  $^1\text{H}$  NMR spectrum of rotaxane **15** (Figure 12) displays signals for the methylene protons adjacent to the ammonium site in the linear guest and  $\alpha$ - and  $\beta$ -protons of the crown ether that are shifted downfield as in the semirotaxane **12** and likewise the  $\gamma$ -protons are shifted upfield (Figure 7). Note also that, as expected because of the asymmetry of the linear guest,<sup>52,53</sup> the ethyleneoxy protons on the two diastereotopic faces of the crown ether are now non-equivalent and each set now is split into two groups, e. g.,  $\text{H}_{\alpha_1}$  and  $\text{H}_{\alpha_2}$ , for the eight  $\alpha$ -protons. In retrospect note that this same situation obtains in the case of rotaxane **14**; however, the two sides of the guest ammonium species are both aromatic and this apparently leads to lack of a large difference between the two faces of the crown ether, whereas with **15** one side of the guest is aromatic and the other is aliphatic.

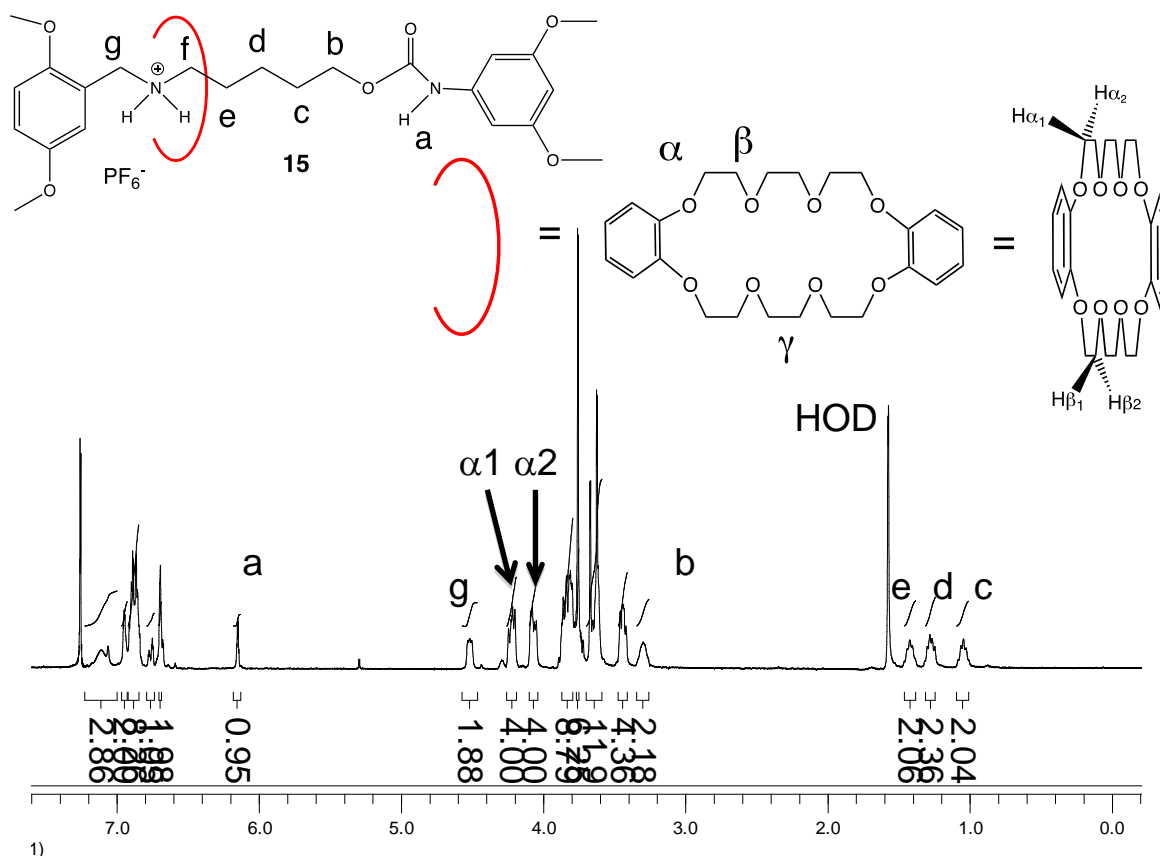


**Figure 12.**  $^1\text{H}$  NMR spectrum (400 MHz,  $\text{CDCl}_3$ ) of [2]rotaxane **15**.

## Conclusions

New secondary ammonium salts were complexed with dibenzo-24-crown-8 to form [2]semirotaxanes and converted to [2]rotaxanes. The formation of [2]semirotaxanes can be turned off and on by adding  $KPF_6$  and 18-crown-6, respectively. [2]Rotaxane **14** was synthesized from hydroxyl-functionalized guest **5a** and **DB24C8** using a thermodynamically driven approach to form the stable trityl ether product, although in disappointingly low yield partly perhaps due to the small reaction scale. Hydroxyl-functionalized secondary ammonium salt **9** with **DB24C8** produced [2]semirotaxane **12**, whose single crystal X-ray analysis confirmed its structure. The corresponding [2]rotaxane **15** was prepared in satisfactory yield by reaction with 3,5-dimethoxyphenyl isocyanate. The use of these unsymmetrical guests with mono- (or unsymmetrically) substituted dibenzo-24-crown-8 derivatives will afford planar chiral [2]rotaxanes and related supramolecular systems.

## Experimental Section

**General.** All starting materials were used as received from commercial sources. All solvents were HPLC grade. Melting points were taken in capillary tubes and are uncorrected.  $^1H$  NMR spectra were obtained on 400 MHz Varian or Inova or JEOL Eclipse Plus 500 MHz spectrometers with tetramethylsilane as an internal standard;  $^{13}C$  NMR spectra were obtained on the same instruments. Elemental analyses were performed by Atlantic Microlabs of Norcross, GA. High resolution fast atom bombardment mass spectra (HR FAB MS) were obtained on a JEOL Model HX 110. Electrospray ionization (ESI) mass spectrometry utilized Agilent HP121 and HP921 TOF instruments using acetonitrile as solvent.

***p*-(2'-Hydroxyethoxy)benzaldehyde (2).** 4-Hydroxybenzaldehyde (**1**, 10.00 g, 0.0819 mol) and 2-chloroethanol (6.09 mL, 0.0909 mol) were added with 95% ethanol (215 mL) to a 500 mL round bottom flask equipped with magnetic stirrer and condenser. Potassium carbonate (15.89 g, 0.115 mol) was added and the mixture was refluxed for 3 days. The solvent was removed to yield a viscous yellow oil, which was dissolved in ethyl acetate and washed with water (3 x 100 mL), 10% NaOH (3 x 75 mL), water (2 x 75 mL), and brine. The organic layer was dried over sodium sulfate. The solvent was removed to yield a viscous yellow oil, 11.74 g (86%). Vicens et al. obtained the product as a yellow oil in 62% yield using acetonitrile as solvent.<sup>54</sup>  $^1H$  NMR (400 MHz,  $CDCl_3$ , ambient T, Figure S1)  $\delta$  (ppm): 9.9 (s, 1H), 7.85 (d, *J* 9, 2H), 7.05 (d, *J* 9, 2H), 4.2 (t, *J* 4, 2H), 4.0 (t, *J* 4, 2H). HR FAB MS (Figure S2):  $[M + H]^+$  *m/z* 167.0705 (calcd. for  $C_9H_{10}O_3$  *m/z* 167.0703, error 1 ppm).

***p*-(2'-Hydroxyethoxy)benzylidene-3'',5''-dimethoxybenzylamine (3).** *p*-(2'-Hydroxyethoxy)benzaldehyde (**2**) (20.92 g, 0.126 mol) and toluene (450 mL) were added to a 1 L round bottom flask equipped with Dean-Stark trap, condenser and nitrogen inlet. 3,5-Dimethoxybenzylamine (21.07 g, 0.126 mol) and tosylic acid (<0.01 g) were added to the solution and the mixture was refluxed for 36 h. The solvent was removed via rotoevaporation to yield an off-white solid, which was recrystallized from hexane/ethyl acetate to yield an off-white crystalline solid, 38.10 g (96%), mp 92-96 °C.  $^1H$  NMR (400 MHz,  $CDCl_3$ , ambient T, Figure S3)  $\delta$  (ppm): 8.4 (s, 1H), 7.83 (d, *J* 9, 2H), 7.05 (d, *J* 9, 2H), 6.60 (d, *J* 2, 2H), 6.43 (t, *J* 2, 1H), 4.75 (s, 2H), 4.25 (t, *J* 4, 2H), 4.00 (t, *J* 4, 2H), 3.70 (s, 6H). Elem. anal., calcd. for  $C_{18}H_{21}NO_4$ : C 68.55; H 6.73; N 4.44; found (duplicate): C 68.61, 68.52; H 6.76, 6.67; N 4.36, 4.48.

***N*-[*p*-(2'-Hydroxyethoxy)benzyl]-3'',5''-dimethoxybenzylamine (4).** Schiff base **3** (2.00 g, 6.34 mmol) and methanol (30 mL) were added to a 50 mL round bottom flask equipped with a magnetic stirrer. Sodium borohydride (0.480 g, 12.7 mmol) was added slowly to the solution and the mixture was refluxed for 16 h. The solvent was removed via rotoevaporation to yield a white solid. The solid was suspended in water and

extracted with  $\text{CHCl}_3$  twice. The organic layers were combined, washed with brine, dried over  $\text{Na}_2\text{SO}_4$  and concentrated to afford a light yellow liquid that solidified upon standing. The product was recrystallized from ethyl acetate, 1.83 g (91%), mp 92-93 °C.  $^1\text{H}$  NMR (400 MHz,  $\text{CDCl}_3$ , ambient T, Figure S4)  $\delta$  (ppm): 7.27 (d,  $J$  9, 2H), 6.90 (d,  $J$  9, 2H), 6.51 (d,  $J$  2, 2H), 6.35 (t,  $J$  2, 1H), 4.10 (t,  $J$  4, 2H), 3.95 (t,  $J$  4, 2H), 3.30 (s, 6H), 3.32 (s, 4H). Elem. anal., calcd. for  $\text{C}_{18}\text{H}_{23}\text{NO}_4$ : C 68.12; H 7.30; N 4.41; found (duplicate): C 68.22, 68.29; H 7.43, 7.28; N 4.51, 4.42.

***N*-[*p*-(2'-Hydroxyethoxy)benzyl]-3'',5''-dimethoxybenzyl ammonium tetrafluoroborate (5a).** Secondary amine **4** (1.83 g, 5.77 mmol) was partially dissolved in ethyl ether/ethyl acetate and  $\text{HBF}_4$  (54 wt. % in  $\text{Et}_2\text{O}$ ) (1.19 mL, 1.41 g, 8.65 mmol) was added to the solution. A precipitate formed. The mixture was stirred 24 h and filtered to yield a light yellow solid, 1.66 g (71%), mp 102-105 °C.  $^1\text{H}$  NMR (400 MHz,  $\text{CD}_3\text{CN}$ , ambient T, Figure S5)  $\delta$  (ppm): 7.41 (d,  $J$  9, 2H), 7.05 (d,  $J$  9, 2H), 6.61 (d,  $J$  2, 2H), 6.58 (t,  $J$  2, 1H), 4.20 (t,  $J$  6, 2H), 4.13 (t,  $J$  6, 2H), 4.09 (t,  $J$  4, 2H), 3.80 (m, 8H). HR FAB MS (Figure S6):  $[\text{M} - \text{BF}_4]^+$   $m/z$  318.1714 (calcd. for  $\text{C}_{18}\text{H}_{24}\text{NO}_4$   $m/z$  318.1700, error 4.4 ppm).

***N*-*p*-(2'-Hydroxyethoxy)benzyl-3'',5''-dimethoxybenzyl ammonium hexafluorophosphate (5b).** Secondary amine (**4**) (5.00 g, 0.0158 mol) was added to 2M HCl (12 mL, 0.024 mol) and a precipitate immediately formed. The mixture was stirred under nitrogen for 2 days and rotoevaporated to yield a light brown solid (mp 85-87 °C), which was dissolved in water and  $\text{NH}_4\text{PF}_6$  was added until no more product precipitated. The off-white product was filtered and dried in a drying pistol, 7.15 g (98%), mp 122-125 °C.  $^1\text{H}$  NMR (400 MHz,  $\text{CD}_3\text{CN}$ , ambient T, Figure S7)  $\delta$  (ppm): 7.42 (d,  $J$  9, 2H), 7.0, (d,  $J$  9, 2H), 6.64 (d,  $J$  2, 2H), 6.59 (t,  $J$  2, 1H), 4.23 (m, 4H), 4.09 (t,  $J$  4, 2H), 3.84 (t,  $J$  4, 2H), 3.8 (s, 6H). HR FAB MS (Figure S8):  $[\text{M} - \text{PF}_6]^+$   $m/z$  318.1699 (calcd. for  $\text{C}_{18}\text{H}_{24}\text{NO}_4$   $m/z$  318.1700, error 0.3 ppm).

**5-[(2',5'-Dimethoxybenzylidene)amino]pentanol (7).** 2,5-Dimethoxybenzaldehyde (2.0 g, 12 mmol) was dissolved in toluene (20 mL) and the solution was put into a 500 mL flask equipped with a condenser and a Dean-Stark trap. 5-Amino-1-pentanol (1.2 g, 12 mol) in toluene (5 mL) was added to the flask dropwise. The solution was refluxed for 2 days. The solvent was removed and a brown oil was obtained. A short silica gel column was used to purify the crude product, yielding a yellow oil (2.90 g, 96%).  $^1\text{H}$ -NMR ( $\text{CDCl}_3$ , 500 MHz, Figure S9):  $\delta$  8.64 (s, 1H), 7.46 (d,  $J$  3 Hz, 1H), 6.93 (m, 1H), 6.83 (d,  $J$  8 Hz, 1H), 3.80 (s, 3H), 3.78 (s, 3H), 3.62 (m, 4H), 2.31(s, 1H), 1.72 (m, 2H), 1.59 (m, 2H). ESI MS (Figure S10):  $[\text{M}]^+$   $m/z$  251.1521 (calcd. for  $\text{C}_{14}\text{H}_{21}\text{NO}_3$  251.1521, error: 0 ppm).

**5-(2',5'-Dimethoxybenzyl)aminopentanol (8).** Schiff base **7** (2.8 g, 11 mmol) was dissolved in MeOH (20 mL).  $\text{NaBH}_4$  (1.0 g, 28 mmol) was added **slowly** to the solution *in small portions (important!)*. The solution was refluxed for 20 h and the solvent was removed. The product was partitioned between  $\text{H}_2\text{O}$  and DCM; the aqueous phase was washed with DCM. The combined organic phase was washed with  $\text{H}_2\text{O}$  and NaCl (aq. sat.) and dried over  $\text{Na}_2\text{SO}_4$ . After solvent was removed, a yellow oil was obtained (2.64 g, 94%).  $^1\text{H}$ -NMR ( $\text{CDCl}_3$ , 500 MHz, Figure S11):  $\delta$ : 6.80 (d,  $J$  3 Hz, 1H), 6.76 (m, 2H), 3.76 (s, 3H), 3.74 (s, 3H), 3.71 (s, 2H), 3.56 (t,  $J$  6 Hz), 2.57 (t,  $J$  6 Hz), 1.53 (m, 4H), 1.37 (m, 2H). ESI MS (Figure S12):  $[\text{M}]^+$   $m/z$  253.1678 (calcd. for  $\text{C}_{14}\text{H}_{23}\text{NO}_3$  253.1678, error: 0 ppm).

***N*-(5'-Hydroxypentyl)-2,5-dimethoxybenzylammonium hexafluorophosphate (9).**  $\text{N}_2$  gas was bubbled through a flask containing HCl (37% aq.) and then into an ethyl acetate (EA) solution of amine **8** (5.0 g, 20 mmol) for 3 h. The white solid that precipitated was collected by filtration and washed with EA. The solid was dissolved in DI  $\text{H}_2\text{O}$  and excess  $\text{NH}_4\text{PF}_6$  (9.67 g, 59.2 mmol) was added. The resulting precipitate was collected, washed with DI  $\text{H}_2\text{O}$  and dried in a vacuum oven: 6.3 g (81%) of colorless solid, mp 85.0-86.0 °C.  $^1\text{H}$ -NMR ( $\text{CD}_3\text{CN}$ , 500 MHz, Figure S13):  $\delta$  7.00 (m, 2H), 6.93 (d,  $J$  3 Hz), 4.12 (s, 2H), 3.85 (s, 3H), 3.76 (s, 3H), 3.51 (t,  $J$  6 Hz, 2H), 3.01 (t,  $J$  6 Hz, 2H), 1.71 (m, 2H), 1.53 (m, 2H), 1.40 (m, 2H).  $^{13}\text{C}$ -NMR ( $\text{CD}_3\text{CN}$ , 125 MHz, Figure S14):  $\delta$



153.62, 151.94, 119.20, 117.67, 115.72, 111.89, 61.20, 55.64, 55.50, 47.94, 47.72, 31.56, 25.16, 22.48. ESI MS (Figure S15):  $[M - PF_6]^+$   $m/z$  254.1756 (calcd. for  $C_{14}H_{24}NO_3$ , 254.1751, error: 2 ppm).

**Semirotaxane 12:** ESI MS of an equimolar solution of **DB24C8** and **9** (Figure S18):  $[M - PF_6]^+$   $m/z$  702.3847 (calcd. for  $C_{38}H_{56}NO_{11}$  702.3848, error: 0.1 ppm).

***N-p*-(2'-Triphenylmethoxyethoxy)benzyl-3'',5''-dimethoxybenzylamine (13).** Ammonium tetrafluoroborate salt **5a** (0.200 g, 0.494 mmol), trityl tetrafluoroborate (0.165 g, 0.593 mmol), and  $CHCl_3/CH_3CN$  (0.75 mL, 1/1) were added to a 5 mL round bottom flask and stirred at room temperature for ~24 h. The solvent was removed to yield a viscous yellow product. The product was treated with 10% NaOH and then dissolved in  $CHCl_3$  and washed with 10% NaOH<sub>(aq)</sub> (3 x 3 mL) and water (2 x 3 mL). More chloroform was added. The product precipitated and the solvent was decanted off to yield a white residue, 0.12 g (39%), mp 155-157 °C.  $^1H$  NMR (400 MHz,  $CD_3CN$ , ambient T),  $\delta$  (ppm): 7.62 (d,  $J$  8, 6H), 7.50 – 7.21 (m, 19H), 7.05 (d,  $J$  9, 2H), 6.61 (d,  $J$  2, 2H), 6.58 (t,  $J$  2, 1H), 4.2 (t,  $J$  6, 2H), 4.13 (t,  $J$  6, 2H), 4.09 (t,  $J$  4, 2H), 3.8 (m, 8H). HR FAB MS (Figure S19):  $[M + H]^+$   $m/z$  560.2807 (calcd. for  $C_{37}H_{38}NO_4$   $m/z$  560.2796, error 2.0 ppm).

**Rotaxane 14.** Ammonium tetrafluoroborate salt **5a** (0.200 g, 0.494 mmol), trityl tetrafluoroborate (0.165 g, 0.593 mmol), **DB24C8** (0.266 g, 0.593 mmol) and  $CHCl_3/CH_3CN$  (0.75 mL, 1/1) were added to a 5 mL round bottom flask and stirred at room temperature for 24 h. The solvent was removed to yield a tacky viscous product that was dissolved in  $CHCl_3$  and washed with 10% NaOH<sub>(aq)</sub> (3 x 3 mL) and water (2 x 3 mL). The solvent was evaporated from the organic phase and the white crystalline product was dried under vacuum, 0.17 g (32%), mp 130-132 °C.  $^1H$  NMR (400 MHz,  $CD_3CN$ , ambient T)  $\delta$  (ppm): 7.62 (d,  $J$  8, 6H), 7.60 – 7.20 (m, 13H), 7.0-6.8 (m, 8H), 6.68 (d,  $J$  8, 2H), 6.54 (d,  $J$  2, 2H), 6.27 (t,  $J$  2, 1 H), 4.70 (bs, 2 H), 4.57 (bs, 2 H), 4.10 (m, 8 H), 3.91 (t,  $J$  8, 2H), 3.81 (m, 10H), 3.71 (M, 8H), 3.60 (m, 6H); small signals at 7.50, 7.02 and 6.61 correspond to signals in dumbbell **13**, indicating its presence as an impurity. HR FAB MS (Figure S20):  $[M - BF_4]^+$   $m/z$  1008.4884 (calcd. for  $C_{61}H_{70}NO_{12}$  1008.4893, error 0.9 ppm).

**[2]Rotaxane 15.** Ammonium salt **9** (300 mg, 0.751 mmol) and **DB24C8** (352 mg, 0.786 mmol) were dried in a vacuum drying pistol with  $P_2O_5$  at 65 °C overnight. The solid mixture was dissolved in DCM (20 mL) and stirred under  $N_2$  for 10 h. 3,5-Dimethoxyphenyl isocyanate (161 mg, 0.899 mmol) and di(*n*-butyl)tin dilaurate (51.5  $\mu$ l) were added to the solution, which was stirred at RT for 2 days. The mixture was submitted to a silica gel column (hexanes/EA 1/1, then DCM:MeOH 97/3) and a waxy solid (585 mg, 76%) was obtained, mp 64.0-65.0 °C.  $^1H$ -NMR ( $CDCl_3$ , 400 MHz):  $\delta$ : 7.13 (br, 3H), 6.95 (s, 2H), 6.90 (m, 8H), 6.75 (m,  $J$  3 Hz, 1H), 6.70 (m, 2H,  $H_2$ ), 6.15 (d,  $J$  3 Hz, 1H), 4.53 (s, 2H), 4.25 (m, 4H), 4.09 (m, 4H), 3.86 (m, 8H), 3.76 (s, 6H), 3.67 (m, 12H), 3.46 (m, 4H), 3.31 (m, 2H), 1.42 (m, 2H), 1.30 (m, 2H), 1.08 (m, 2H).  $^{13}C$ -NMR (100 MHz,  $CDCl_3$ , Figure S24):  $\delta$  161.05, 153.52, 153.16, 151.55, 147.46, 140.10, 121.62, 121.14, 117.57, 114.83, 112.50, 111.14, 96.54, 95.68, 77.25, 77.00, 76.74, 70.72, 70.18, 68.00, 64.21, 55.57, 55.37, 55.36, 49.13, 48.20, 28.11, 25.84, 22.74. 29.76 (grease). ESI MS (Figure S25):  $[M - PF_6]^+$   $m/z$  881.4417 (calcd. for  $C_{47}H_{65}N_2O_{14}$  881.4430, error: 1.5 ppm).

## Acknowledgements

This work was supported by the National Science Foundation (DMR0097126, DMR0704076) and the Petroleum Research Fund administered by the American Chemical Society (47644-AC). We also acknowledge the National Science Foundation for funds to purchase the Innova-400 MHz NMR and the Agilent 6220 Accurate Mass TOF LC/MS Spectrometers (CHE-0131124 & CHE-0722638, respectively).



## Supplementary Material

$^1\text{H}$  (including COSY) and  $^{13}\text{C}$  NMR spectra, mass spectra and crystallographic details on semirotaxane **12**.

## References

1. Deska, M.; Kozłowska, J.; Sliwa, W. *Arkivoc* **2013**, (i), 294-332.  
<https://doi.org/10.3998/ark.5550190.p007.774>
2. Xue, M.; Yang, Y.; Chi, X.; Yan, X.; Huang, F. *Chem. Rev.* **2015**, *115*, 7398-7501.  
<https://doi.org/10.1021/cr5005869>
3. Ghosh, S.; Mukhopadhyay, C. *J. Incl. Phen. Macrocyc. Chem.* **2017**, *88*, 105-128.  
<https://doi.org/10.1007/s10847-017-0725-5>
4. Han, Z.; Zhou, Q.; Li, Y. *J. Incl. Phen. Macrocyc. Chem.* **2018**, *92*, 81-101.  
<https://doi.org/10.1007/s10847-018-0828-7>
5. Yang, K.; Chao, S.; Zhang, F.; Pei, Y.; Pei, Z. *Chem. Commun.* **2019**, *55*, 13198-13210.  
<https://doi.org/10.1039/C9CC07373F>
6. Gibson, H. W.; Bheda, M. C.; Engen, P. T. *Prog. Polym. Sci.* **1994**, *19*, 843-945.  
[https://doi.org/10.1016/0079-6700\(94\)90034-5](https://doi.org/10.1016/0079-6700(94)90034-5)
7. Harada, A.; Takashima, Y.; Yamaguchi, H. *Chem. Soc. Rev.* **2009**, *38*, 875-882.  
<https://doi.org/10.1039/b705458k>
8. Niu, Z.; Gibson, H. W. *Chem. Rev.* **2009**, *109*, 6024-6046.  
<https://doi.org/10.1021/cr900002h>
9. Arunachalam, M.; Gibson, H. W. *Progr. Polym. Sci.* **2014**, *39*, 1043-1073.  
<https://doi.org/10.1016/j.progpolymsci.2013.11.005>
10. Jamieson, E. M. G.; Modicom, F.; Goldup, S. M. *Chem. Soc. Rev.* **2018**, *47*, 5266-5311.  
<https://doi.org/10.1039/C8CS00097B>
11. Liu, Y.; O'Keeffe, M.; Treacy, M. M. J.; Yaghi, O. M. *Chem. Soc. Rev.* **2018**, *47*, 4642-4664.  
<https://doi.org/10.1039/C7CS00695K>
12. Mena-Hernando, S.; Perez, E. M. *Chem. Soc. Rev.* **2019**, *48*, 5016-5032.  
<https://doi.org/10.1039/C8CS00888D>
13. Leigh, D. A.; Lewandowska, U.; Lewandowski, B.; Wilson, M. R. *Topics Curr. Chem.* **2014**, *354*, 111-138.  
[https://doi.org/10.1007/128\\_2014\\_546](https://doi.org/10.1007/128_2014_546)
14. Wang, F.; Willner, B.; Willner, I. *Topics Curr. Chem.* **2014**, *354*,
15. Niess, F.; Duplan, V.; Sauvage, J.-P. *Chem. Lett.* **2014**, *43*, 964-974.  
<https://doi.org/10.1246/cl.140315>
16. Kassem, S.; van Leeuwen, T.; Lubbe, A. S.; Wilson, M. R.; Feringa, B. L.; Leigh, D. A. *Chem. Soc. Rev.* **2017**, *46*, 2592-2621.  
<https://doi.org/10.1039/C7CS00245A>
17. Pezzato, C.; Cheng, C.; Stoddart, J. F.; Astumian, R. D. *Chem. Soc. Rev.* **2017**, *46*, 5491-5507.  
<https://doi.org/10.1039/C7CS00068E>
18. Venturi, M.; Iorga, M. I.; Putz, M. V. *Curr. Org. Chem.* **2017**, *21*, 2731-2759.  
<https://doi.org/10.2174/1385272821666170531121733>
19. Goujon, A.; Moulin, E.; Fuks, G.; Giuseppone, N. *CCS Chemistry* **2019**, *1*, 83-96.
20. Cheng, C.-A.; Deng, T.; Lin, F.-C.; Cai, Y.; Zink, J. I. *Theranostics* **2019**, *9*, 3341-3364.

<https://doi.org/10.7150/thno.34576>

21. Astumian, R. D.; Pezzato, C.; Feng, Y.; Qiu, Y.; McGonigal, P. R.; Cheng, C.; Stoddart, J. F. *Mater. Chem. Frontiers* **2020**, *4*, 1304-1314.  
<https://doi.org/10.1039/D0QM00022A>
22. Qiu, Y.; Song, B.; Pezzato, C.; Shen, D.; Liu, W.; Zhang, L.; Feng, Y.; Guo, Q.-H.; Cai, K.; Li, W.; et al. *Science* **2020**, *368*, 1247-1253.  
<https://doi.org/10.1126/science.abb3962>
23. La Cognata, S.; Miljkovic, A.; Mobili, R.; Bergamaschi, G.; Amendola, V. *ChemPlusChem* **2020**, *85*, 1145-1155.  
<https://doi.org/10.1002/cplu.202000274>
24. Baroncini, M.; Silvi, S.; Credi, A. *Chem. Rev.* **2020**, *120*, 200-268.  
<https://doi.org/10.1021/acs.chemrev.9b00291>
25. Koyama, Y. *Polym. J.* **2014**, *46*, 315-322.  
<https://doi.org/10.1038/pj.2014.9>
26. Takata, T. *Bull. Chem. Soc. Jpn.* **2019**, *92*, 409-426.  
<https://doi.org/10.1246/bcsj.20180330>
27. Sobransingh, D.; Kaifer, A. E. *Org. Lett.* **2006**, Vol. 8, 3247.  
<https://doi.org/10.1021/ol061128+>
28. Ma, X.; Sun, R.; Li, W.; Tian, H. *Polym. Chem.* **2011**, *2*, 1068-1070.  
<https://doi.org/10.1039/c0py00419g>
29. Jones, J. W.; Bryant, W. S.; Bosman, A. W.; Janssen, R. A. J.; Meijer, E. W.; Gibson, H. W. *J. Org. Chem.* **2003**, *68*, 2385-2389.  
<https://doi.org/10.1021/jo0265784>
30. Huang, F. H.; Switek, K. A.; Gibson, H. W. *Chem. Commun.* **2005**, 3655-3657.  
<https://doi.org/10.1039/b504250j>
31. Sindelar, V.; Silvi, S.; Kaifer, A. E. *Chem. Commun.* **2006**, 2185-2187.  
<https://doi.org/10.1039/b601959e>
32. Murakami, H.; Kawabuchi, A.; Kotoo, K.; Kunitake, M.; Nakashima, N. *J. Am. Chem. Soc.* **1997**, *119*, 7605-7606.  
<https://doi.org/10.1021/ja971438a>
33. Qu, D. H.; Wang, Q. C.; Ren, J.; Tian, H. *Org. Lett.* **2004**, *6*, 2085-2088.  
<https://doi.org/10.1021/ol049605g>
34. Ashton, P. R.; Chrystal, E. J. T.; Glink, P. T.; Menzer, S.; Schiavo, C.; Spencer, N.; Stoddart, J. F.; Tasker, P. A.; White, A. J. P.; Williams, D. J. *Chem. Eur. J.* **1996**, *2*, 709-728.  
<https://doi.org/10.1002/chem.19960020616>
35. Aston, P. R.; Fyfe, M. C. T.; Hickingbottom, S. K.; Stoddart, J. F.; White, A. J. P.; Williams, D. J. *J. Chem. Soc. Perkin Trans. 2* **1998**, 2117-2128.  
<https://doi.org/10.1039/a802406e>
36. Yamamoto, C.; Okamoto, Y.; Schmidt, T.; Jäger, R.; Vögtle, F. *J. Am. Chem. Soc.* **1997**, *119*, 10547-10548.  
<https://doi.org/10.1021/ja971764q>
37. Reuter, C.; Schmieder, R.; Vögtle, F. *Pure Appl. Chem.* **2000**, *72*, 2233-2241.  
<https://doi.org/10.1351/pac200072122233>
38. Makita, Y.; Kihara, N.; Nakakoji, N.; Takata, T.; Inagaki, S.; Yamamoto, C.; Okamoto, Y. *Chem. Lett.* **2007**, *36*, 162-163.

- <https://doi.org/10.1246/cl.2007.162>
39. Glen, P. E.; O'Neill, J. A. T.; Lee, A.-L. *Tetrahedron* **2013**, *69*, 57-68.  
<https://doi.org/10.1016/j.tet.2012.10.069>
40. Cantrill, S. J.; Rowan, S. J.; Stoddart, J. F. *Org. Lett.* **1999**, *1*, 1363-1366.  
<https://doi.org/10.1021/ol990966j>
41. Rowan S. J.; Stoddart, J. F. *Org. Lett.*, **1999**, *1*, 1913-1916.  
<https://doi.org/10.1021/ol991047w>
42. Glink, P. T.; Oliva, A. I.; Stoddart, J. F.; White, A. J. P.; Williams, D. J. *Angew. Chem., Int. Ed.* **2001**, *10*, 1870-1875.  
[https://doi.org/10.1002/1521-3773\(20010518\)40:10<1870::AID-ANIE1870>3.0.CO;2-Z](https://doi.org/10.1002/1521-3773(20010518)40:10<1870::AID-ANIE1870>3.0.CO;2-Z)
43. Furusho, Y.; Rajkumar, G. A.; Oku, T.; Takata, T. *Tetrahedron* **2002**, *58*, 6609-6613.  
[https://doi.org/10.1016/S0040-4020\(02\)00749-4](https://doi.org/10.1016/S0040-4020(02)00749-4)
44. Furusho, Y.; Oku, T.; Rajkumar, G. A.; Takata, T. *Chem. Lett.* **2004**, *33*, 52-53.  
<https://doi.org/10.1246/cl.2004.52>
45. Furusho, Y.; Oku, T.; Hasegawa, T.; Tsuboi, A.; Kihara, N.; Takata, T. *Chem. Eur. J.* **2003**, *9*, 2895.  
<https://doi.org/10.1002/chem.200204644>
46. Oku, T.; Furusho, Y.; Takata, T. *J. Polym. Sci. Part A: Polym. Chem.* **2003**, *41*, 119.  
<https://doi.org/10.1002/pola.10571>
47. Tokunaga, Y.; Kakuchi, S.; Akasaka, K.; Nishikawa, N.; Shimomura, Y.; Isa, K.; Seo, T. *Chem. Lett.* **2002**, 810-811.  
<https://doi.org/10.1246/cl.2002.810>
48. Jones, J. W.; Gibson, H. W. *J. Am. Chem. Soc.* **2003**, *23*, 7001-7004.  
<https://doi.org/10.1021/ja034442x>
49. Gibson, H. W.; Jones, J. W.; Zakharov, L. N.; Rheingold, A. L.; Sleboznick, C. *Chem. Eur. J.* **2011**, *17*, 3192-3206.  
<https://doi.org/10.1002/chem.201002522>
50. Gibson, H. W.; Wang, H.; Bonrad, K.; Jones, J. W.; Sleboznick, C.; Habenicht, B.; Lobue, P. *Org. Biomol. Chem.* **2005**, *3*, 2114-2121.  
<https://doi.org/10.1039/b503072m>
51. Kihara, N.; Tachibana, Y.; Kawasaki, H.; Takata, T. *Chem. Lett.* **1999**, *29*, 506-507.  
<https://doi.org/10.1246/cl.2000.506>
52. Cantrill, S. J.; Fulton, D. A.; Heiss, A. M.; Pease, A. R.; Stoddart, J. F.; White, A. J. P.; Williams, D. J. *Chem. Eur. J.* **2000**, *6*, 2274-2287.  
[https://doi.org/10.1002/1521-3765\(20000616\)6:12<2274::AID-CHEM2274>3.0.CO;2-2](https://doi.org/10.1002/1521-3765(20000616)6:12<2274::AID-CHEM2274>3.0.CO;2-2)
53. Nakazono, K.; Oku, T.; Takata, T. *Tetrahedron Lett.* **2007**, *48*, 3409-3411.  
<https://doi.org/10.1016/j.tetlet.2007.03.064>
54. Aeungmaitrepirom W.; Asfari Z.; Vicens J. *Tetrahedron Lett.* **1997**, *38*, 1907-1910.  
[https://doi.org/10.1016/S0040-4039\(97\)00240-2](https://doi.org/10.1016/S0040-4039(97)00240-2)

This paper is an open access article distributed under the terms of the Creative Commons Attribution (CC BY) license (<http://creativecommons.org/licenses/by/4.0/>)